# Ballistic Behavior of Solid Propellant Grains under High Acceleration

Z. H. LANDAU* AND J. M. CEGIELSKI†
*Douglas Aircraft Company, Inc., Santa Monica, Calif.*

**Successful development of vehicles with high acceleration requires determination of the effects of acceleration on solid-propellant burning rate and grain ballistic history. This paper describes tests of case-bonded, cylindrically ported, aluminized composite propellant grains under accelerations as high as 200 $g$. Data for centrifuge-mounted motors containing 3 lb and 100 lb of propellant burning at 1000–2000 psia are evaluated statistically. In contrast to the results of some previous investigators, no deleterious effects on combustion process were noted for either lateral or longitudinal accelerations.**

## Nomenclature

$A$ = area, ft²
$A_b$ = propellant burning surface area, ft²
$a$ = acceleration (environment), ft/sec²
$b_i$ = statistically evaluated constant
$C_P$ = specific heat at constant pressure, ft-lb/lb-mol-°R
$C^*$ = characteristic velocity, fps
$c$ = coefficient in the burning-rate law
$H$ = enthalpy, ft-lb/lb-mol
$n$ = exponent in the burning-rate law
$P$ = pressure, lb/ft²
$R$ = gas constant, 1545 ft-lb/lb-mol-°R
$r$ = propellant burning rate, fps
$T$ = temperature, °R
$t$ = time, sec
$U$ = velocity, fps
$V_c$ = volume, ft³
$W$ = weight, lb
$\alpha$ = direction of acceleration relative to the longitudinal axis of the motor
$\gamma$ = ratio of specific heats
$\rho$ = density, lb/ft³

### *Subscripts*

$c$ = gas in chamber
$D$ = ignition delay
eq = equilibrium (time)
$p$ = propellant (solid)
$u$ = useful (time)
$T$ = total (time)
$s$ = constant entropy
$H$ = head-end
1, 2 = stations (1 is same as $H$)

### *Superscript*

* = nozzle throat condition

## Introduction

THE advent of high-performance vehicles presents serious problems to the designer of solid-propellant rocket motors. Three possible causes of performance deviation of a solid-propellant grain under acceleration loads can be postulated: 1) deformation of the combustion cavity due to propellant slump (and possible bond failure or spalling); 2) stresses in the macroscopic structure of the propellant which affect the burning rate; and 3) changes in the gas dynamics of the combustion zone coupled with heterogeneous, turbulent convection currents in the chamber. It is important to the designer to be able to evaluate separately the influences of each of the postulated causes of performance deviation. Unfortunately, the nature of these phenomena and the interactions among them greatly complicate the formulation of a reliable analytical technique with which to predict order-of-magnitude effects. This situation suggests a test program aimed at developing empirical design data and answering in a gross manner the following questions related to the third foregoing cause. Does a threshold exist above which acceleration-oriented combustion phenomena effects become noticeable? If so, is it affected by motor-size propellant formulation or an interaction between chamber pressure level and acceleration loading?

Data were obtained by firing 3-lb and 100-lb motors on centrifuges at the Douglas Aircraft Company and the Sandia Corporation. It was recognized that centrifuges do not load the viscoelastic solid propellants in the same manner as a typical launch; however, in search of a threshold for ballistic anomalies, this technique is acceptable for isolating the third postulated cause from the first two. To minimize stresses, deformations, and erosive burning characteristics in the test motors, the motors used had cylindrical port grain geometry, large port-to-throat areas ratio, and small web fractions.

## Experimental Facilities and Procedures

A statistical test pattern was employed to gather data for chamber pressures from 1000 to 2000 psia, accelerations from 100 to 150 $g$, and acceleration orientation from 0° to 90°. Figure 1 illustrates the test pattern selected to provide the necessary statistical data by 15 firings and 4 replication

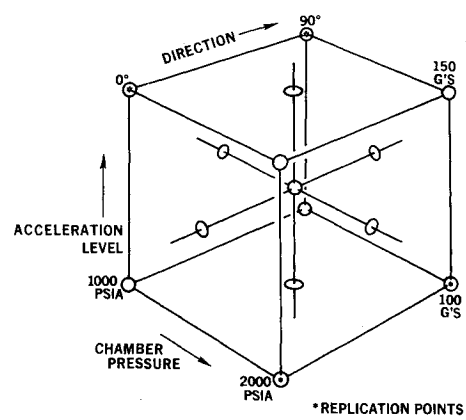


**Fig. 1 Statistical design of dynamic combustion test.**

Presented as Preprint 64-228 at the 1st AIAA Annual Meeting, Washington, D. C., June 29–July 2, 1964; revision received January 22, 1965. The authors wish to acknowledge the advice and technical support of R. W. Froelich and D. K. Wang of the Aerojet-General Corporation; W. C. Aycock and R. P. King of the Thiokol Chemical Corporation, and their associates.

* Propulsion Specialist, Missile and Space Systems Division. Member AIAA.

† Propulsion Engineer, Missile and Space Systems Division. Member AIAA.

points. Three control firings under static conditions were added, thereby bringing the total number of firings required to 22. For this purpose, 25 (including 3 spares) standard ballistic evaluation motors, designation TX-3 (Fig. 2), were supplied by the Thiokol Chemical Corporation. These motors were processed under standard production conditions and loaded from a single batch with approximately 3 lb of aluminized PBAA propellant, formulation TPH-8126, which was case-bonded.

These test firings were conducted on the Douglas centrifuge, which is hydraulically driven and is rated at 150,000 $g$-lb. The 18-ft boom can be rotated at a maximum of 156 rpm under no load. To obtain 150 $g$, the test motor was mounted on an extension platform at the end of the boom, increasing the moment arm to the motor's center of gravity to 19.33 ft. The test installation accommodated the motors in firing positions with their longitudinal axes at 0°, 45°, and 90° relative to the centrifuge axis of rotation. The pressure transducers were dynamically calibrated under pressure and acceleration loads. The transducers were mounted in the test setup with their least sensitive axis appropriately located. Their outputs, firing currents, and voltages were transmitted through an available slip-ring arrangement on the centrifuge to a recording oscillograph at the control center.

Qualitative information rather than statistical measures can provide answers to the question of whether or not the threshold for the acceleration-oriented combustion phenomenon is sensitive to propellant formulation. A small number of firings with different propellant formulations, in addition to the TX-3 tests, would yield sufficient data on this sensitivity factor. For this part of the test program, the Aerojet-General Corporation (AGC) furnished standard ballistic evaluation motors (1-KS-250, Fig. 3) with two different case-bonded, aluminized polyurethane grains: 1.0 lb of formulation ANP2969 (burning rate 0.3 in./sec at 1000 psia), or 2.5 lb of formulation ANP3063 (burning rate, 0.7 in./sec at 1000 psia). The cylindrical port configuration was similar to that in the TX-3 motors, and a similar test setup was used.

Larger motors supplied by AGC for evaluation of the scale-up question had approximately 105 lb of aluminized polyurethane propellant formulation ANP3063 cast and case-bonded in 10-KS-2500 hardware with cylindrical port grain configuration (Fig. 4). Since these motors exceeded the capacity of the Douglas centrifuge facility, the testing was diverted to the Sandia Corporation's hydraulic centrifuge at Albuquerque, N. Mex. which has a 36-ft boom and a capacity of 450,000 $g$-lb.

## Results and Interpretation

Monitoring of the head-end chamber pressure $P_H$ is the standard method of evaluating the ballistic performance of solid-propellant rocket motors. An analysis was performed in order to establish the suitability of $P_H$ for detecting the phenomena sought in these tests.

The result shown in the Appendix indicates that the $P_H$ should be somewhat lower under high axial acceleration than

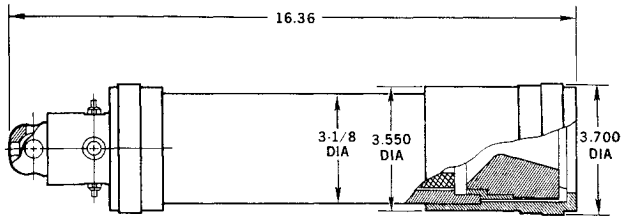


**Fig. 3 1-KS-250 test motor.**

under static conditions (e.g., about 1% lower for 150 $g$ applied for 0.1 sec). However, the expected change in $P_H$ for the test specimens of this program is much smaller because of their extremely short staytime (0.0001 sec). Therefore, if the measured $P_H$ does differ markedly from that obtained from the identical test specimen under static conditions, the deviation can be attributed to acceleration-oriented combustion phenomena.

The results of the ballistic evaluation of the TX-3 statistical firings are summarized in Table 1. The static reference firings are lettered to distinguish them from the numbered rounds fired at the dynamic test conditions. The oscillograph traces of rounds 14–16 showed a progressive deterioration in the quality of the transmitted pressure signal. An investigation revealed that a hydraulic return line was leaking and had sprayed oil on the slip rings, which transmit the pressure signals. A spare motor with the same operating pressure as round 16, designated 16$R$, was used to repeat the test. The results confirmed that the oil leakage had introduced error into the pressure data recorded during the previous three firings; therefore, the pressure data could not be incorporated in the statistical analysis. However, the corresponding time measurements, which are independent of the magnitude of the transmitted pressure signals, could be included. Figure 5 is a composite of the pressure histories from these firings at the respective reference pressure levels.

Superimposed on these figures are the all-inclusive deviations ($3\sigma$) for the TX-3 motors which cover propellant batch-to-batch variation, hardware manufacturing tolerances, instrumentation, and data-reduction errors from many firings over the years. The propellant batch-to-batch variation, which is a major contributor to ballistic variations in rocket motors, was eliminated from the motors of this test program, since they were produced from single batches of propellant mix. It should be expected, therefore, that the standard deviation of the data obtained from this selective sample would be smaller than the all-inclusive one reported by the manufacturers. This has been verified from the replication points of the TX-3 tests yielding the standard deviations shown in Table 2. The pressure traces obtained from the TX-3 motor firings, although exhibiting some spread, did not exhibit drastic deviations in the ballistic performance, and generally fell well within the reported standard deviation ($3\sigma$) limits for these motors. On this basis, it can be concluded that no major anomalies were introduced into the bal-

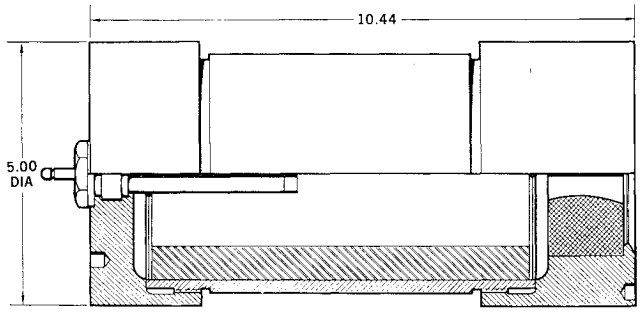


**Fig. 2 TX-3 motor assembly.**

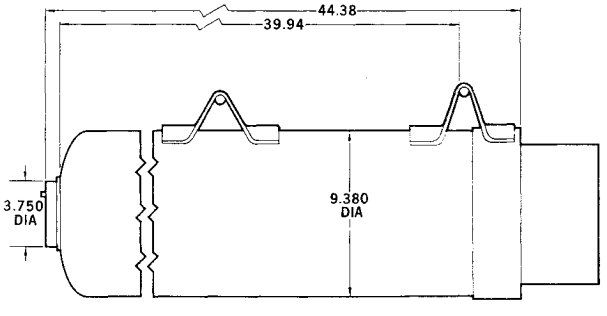


**Fig. 4 10-KS-2500 test motor.**

**Table 1 Ballistic characteristics of test motors**

| Motor no. | $\alpha$ | $P_{avg}$ | $g$ level | $t_D$ | $t_{eq}$ | $t_u$ | $t_T$ | $R_B$ | $\int_{teq}^{} Pdt$ | $\int_{tu}^{} Pdt$ | $\int_{tT}^{} Pdt$ | $\frac{P_{max}}{P_{avg}}$ | $W_p$ | $C^*$ |
|---|---|---|---|---|---|---|---|---|---|---|---|---|---|---|
| A | 0 | 837 | 1.0 | 0.014 | 0.856 | 0.924 | 1.008 | 0.748 | 716 | 750 | 755 | 1.017 | 2.776 | 5004 |
| 1 | 0 | 821 | 101.0 | 0.008 | 0.862 | 0.927 | 0.962 | 0.742 | 708 | 747 | 749 | 1.026 | 2.757 | 5000 |
| 2 | 0 | ... | 101.0 | 0.009 | 0.763 | 0.808 | 0.880 | 0.839 | ... | ... | ... | ... | 2.683 | ... |
| 3 | 0 | 823 | 143.9 | 0.010 | 0.864 | 0.932 | 1.017 | 0.741 | 711 | 748 | 752 | 1.023 | 2.796 | 4971 |
| 4 | 0 | 1360 | 142.9 | 0.014 | 0.750 | 0.805 | 0.888 | 0.853 | 1186 | 1232 | 1235 | 1.199 | 2.771 | 4887 |
| 5 | 0 | 1191 | 125.7 | 0.010 | 0.799 | 0.858 | 0.900 | 0.801 | 952 | 990 | 992 | 1.066 | 2.764 | 4863 |
| 6 | 0 | 1607 | 101.4 | 0.010 | 0.740 | 0.816 | 0.850 | 0.865 | 1190 | 1252 | 1254 | 1.040 | 2.782 | 4936 |
| 7 | 0 | 832 | 142.0 | 0.012 | 0.868 | 0.936 | 1.022 | 0.737 | 722 | 763 | 766 | 1.030 | 2.778 | 5074 |
| B | 45 | 1124 | 1.0 | 0.014 | 0.808 | 0.869 | 0.929 | 0.792 | 908 | 946 | 948 | 1.018 | 2.788 | 4607 |
| 8 | 45 | 1130 | 101.4 | 0.011 | 0.821 | 0.866 | 0.940 | 0.780 | 928 | 952 | 955 | 1.026 | 2.784 | 4648 |
| 9 | 45 | 1137 | 142.7 | 0.010 | 0.790 | 0.874 | 0.931 | 0.810 | 898 | 951 | 955 | 1.032 | 2.796 | 4634 |
| 10 | 45 | 800 | 125.7 | 0.014 | 0.876 | 0.932 | 0.962 | 0.731 | 700 | 745 | 747 | 1.055 | 2.747 | 5016 |
| 11 | 45 | 1599 | 125.7 | 0.008 | 0.748 | 0.814 | 0.865 | 0.856 | 1196 | 1260 | 1262 | 1.037 | 2.767 | 4964 |
| 12 | 45 | 1099 | 125.7 | 0.009 | 0.815 | 0.868 | 0.912 | 0.785 | 897 | 931 | 933 | 1.024 | 2.787 | 4549 |
| C | 90 | 1572 | 1.0 | 0.012 | 0.752 | 0.824 | 0.860 | 0.851 | 1182 | 1234 | 1245 | 1.034 | 2.797 | 4881 |
| 13 | 90 | 832 | 101.4 | 0.010 | 0.873 | 0.935 | 1.00 | 0.733 | 727 | 763 | 766 | 1.038 | 2.781 | 5082 |
| 14 | 90 | ... | 101.4 | 0.015 | 0.755 | 0.814 | 0.880 | 0.848 | ... | ... | ... | ... | 2.757 | ... |
| 15 | 90 | ... | 143.9 | 0.009 | 0.899 | 0.936 | 0.980 | 0.712 | ... | ... | ... | ... | 2.759 | ... |
| 16 | 90 | ... | 143.9 | 0.006 | 0.760 | 0.810 | 0.841 | 0.842 | ... | ... | ... | ... | 2.768 | ... |
| 16R | 90 | 1650 | 143.9 | 0.012 | 0.748 | 0.817 | 0.845 | 0.856 | 1234 | 1294 | 1296 | 1.082 | 2.804 | 5084 |
| 17 | 90 | 1060 | 125.7 | 0.011 | 0.803 | 0.870 | 0.930 | 0.797 | 851 | 1001 | 1003 | 1.160 | 2.798 | 4857 |
| 18 | 90 | 844 | 101.4 | 0.010 | 0.856 | 0.936 | 0.980 | 0.748 | 722 | 776 | 772 | 1.025 | 2.788 | 5107 |
| 19 | 90 | 1655 | 143.9 | 0.010 | 0.732 | 0.818 | 0.850 | 0.874 | 1211 | 1298 | 1301 | 1.065 | 2.829 | 4883 |
| 1-KS-250 motors | | | | | | | | | | | | | | |
| 1 | 0 | 1021 | 1.0 | 0.022 | 1.042 | 1.096 | 1.152 | 0.816 | 1064 | 1112 | 1116 | 1.27 | 2.43 | 5000 |
| 2 | 0 | 1011 | 141.7 | 0.168 | 1.042 | 1.092 | 1.134 | 0.816 | 1054 | 1084 | 1087 | 1.33 | 2.43 | 4870 |
| 3 | 0 | 1043 | 142.1 | 0.012 | 0.960 | 1.056 | 1.096 | 0.885 | 1001 | 1066 | 1069 | 1.26 | 2.43 | 4789 |
| 4 | 0 | 1728 | 1.0 | 0.008 | 0.849 | 0.900 | 0.992 | 1.001 | 1467 | 1496 | 1505 | 1.05 | 2.43 | 3627 |
| 5 | 0 | 1796 | 142.8 | 0.023 | 0.851 | 0.897 | 0.997 | 0.995 | 1528 | 1568 | 1575 | 1.05 | 2.43 | 3796 |
| 6[a] | 0 | 1724 | 142.1 | 0.023 | 0.906 | 0.961 | 0.991 | 0.938 | 1562 | 1604 | 1605 | 1.30 | 2.43 | ... |
| 7 | 0 | 1770 | 141.7 | 0.028 | 0.852 | 0.916 | 0.974 | 0.9976 | 1508 | 1565 | 1572 | 1.06 | 2.43 | 3788 |
| 8 | 19.5 | 1723 | 142.8 | 0.023 | 0.852 | 0.907 | 0.978 | 0.9976 | 1468 | 1506 | 1509 | 1.04 | 2.43 | 3637 |
| 10-KS-2500 motors (Sandia tests) | | | | | | | | | | | | | | |
| 1 | 0 | 1389 | 1 | 0.020 | 2.106 | 2.310 | 2.350 | ... | 2926 | 3085 | 3104 | 1.088 | 104.9 | 4906.9 |
| 2 | 0 | 1363 | 139.8 | 0.013 | 2.142 | 2.279 | 2.322 | ... | 2920 | 3018 | 3022 | 1.110 | 105.9 | 4750.6 |
| 3 | 0 | 1357 | 190.1 | 0.024 | 2.093 | 2.276 | 2.320 | ... | 2840 | 2993 | 2995 | 1.118 | 105.3 | 4707.5 |

[a] Lost nozzle during test.

listic performance of the motors by the acceleration environment. However, since some spread in the data from this selective statistical sample was indicated, the data were analyzed in order to resolve whether the indicated spread was due to the acceleration environment or just the normal experimental error distribution. Since the data were gathered from an experiment with two degrees of freedom (one less than the number of the independent variables), a full quadratic equation can be used to represent the relationship between the chamber pressure $P_H$, acceleration $a$, and direction $\alpha$, and various ballistic parameters:

$$F(g) = b_0 + b_1\alpha + b_2P_H + b_3a + b_4\alpha P_H + b_5\alpha a + b_6P_Ha + b_7\alpha^2 + b_8P_H^2 + b_9a^2$$

The ballistic parameters selected for the statistical evaluation were useful time $t_u$, total time $t_T$, and the useful pressure time integral

$$\int_{tu} P_H dt$$

**Table 2 Standard deviation**

| Parameter | $3\sigma$, % This test | Reported |
|---|---|---|
| Useful time | 1.3 | 4.1 |
| Useful pressure integral | 1.9 | 2.9 |

These parameters are the only ones on which direct measurements were obtained (the centrifuge was not equipped to measure thrust).

The standard multivariate regressive analysis was employed. The standard deviation obtained from the test data was used as an estimate in this regression analysis, which tested the significance of each term in the equation and the over-all ability of the model to represent the data. The results, summarized in Table 3, show that only the pressure terms were significant within the test region. Therefore, the data spread is not indicative of any environmentally induced ballistic anomalies, and it can be concluded that, if a threshold for combustion-oriented acceleration phenomena does indeed exist, it was not reached within the environmental limits of this test.

Four tests with the low-burning-rate polyurethane formulation in the 1-KS-250 motor were performed first. These

**Table 3 Results of regression analysis on the TX-3 test data[a]**

| $F(g)$ | $b_0$ | $b_2$ | $b_8$ | $b_9$ |
|---|---|---|---|---|
| $\int_{tT} P_H dt$ | −21.015 | 1.084 | 0.00017 | 0 |
| $t_u$ | 1.279 | −0.000558 | 0 | 0 |
| $t_T$ | 1.261 | −0.000404 | 0 | 0 |

[a] $F(g) = b_0 + b_1\alpha + b_2P_H + b_3a + b_4\alpha P_H + b_5\alpha a + b_6P_Ha + b_7\alpha^2 + b_8P_H^2 + b_9a^2$; $b_1 = b_3 = b_4 = b_5 = b_6 = b_7 = b_9 = 0$ for all cases; $\int_{tu} P_H dt = \int_{tT} P_H\, dt - 2.5$.

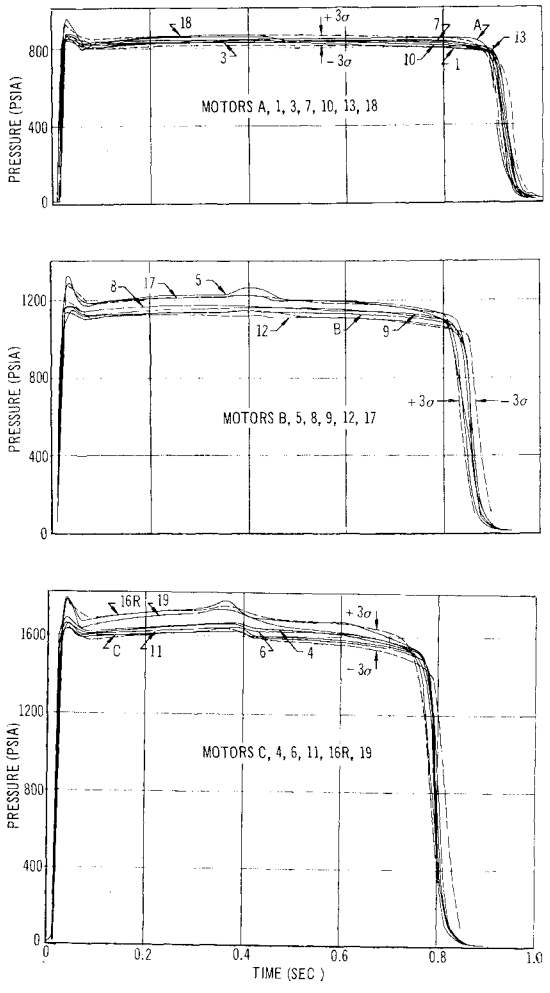


**Fig. 5 Pressure vs time for Thiokol TX-3 test motor. Acceleration: 1 → 144 *g*; orientation: 0° → 90°.**

motors were equipped with soft ignitors to prevent ignition spikes, which could possibly mask data on acceleration-oriented combustion phenomena. The soft ignitors resulted in an ignition delay, bordering on "hang-fire," which was more pronounced with higher acceleration. A clue to the solution of this problem was found when the ignition delay times at the two pressure levels were compared. It was discovered that the higher pressure motors with the smaller throats exhibited shorter ignition delays under all acceleration levels than did the motors with the low chamber pressure and larger throats. In subsequent tests of these motors, harder ignitors were used and ignition delays of the order of 0.006 to

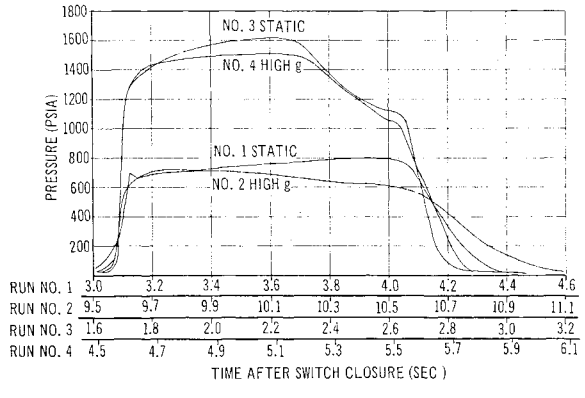


**Fig. 6 First series of tests of 1-KS-250 test motor. Acceleration: 1 → 157.2 *g*.**

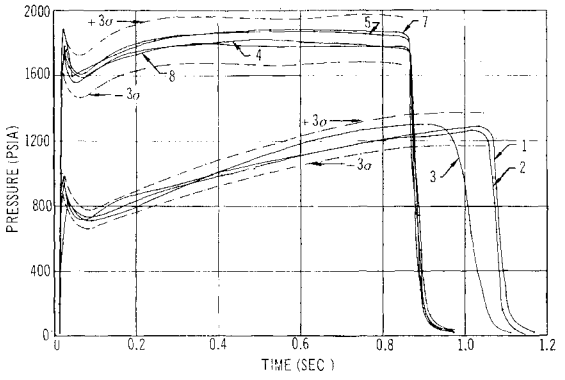


**Fig. 7 Second series of tests of 1-KS-250 test motor. Acceleration: 1 → 145 *g*; orientation: 0° → 19.5°.**

0.015 sec were achieved under all acceleration conditions. Although the data from this set of motors, shown in Fig. 6, appeared to be affected greatly by poor ignition, the general shape of the pressure-time traces was reproduced fairly well under high acceleration conditions. The variations in these traces are due mainly to the low-level burning of the main propellant during the long ignition periods.

The results from the second set of 1-KS-250 motors with higher-burning-rate aluminized polyurethane propellant are summarized in Table 1. Figure 7 is a composite pressure history of these motors at their respective pressure levels; the reported standard deviation ($3\sigma$) limits for these motors are superimposed. It can be seen that the data fell well within these limits and that the shapes of the traces did not exhibit marked deviations from those of the control traces obtained under static conditions. Therefore, it can be stated that the acceleration environment did not cause significant ballistic anomalies. Furthermore, since no anomalies were observed for either of the two propellants, it can be stated that no sensitivity to propellant formulation (or burning rate) in the acceleration environment was detected within the test region.

The ballistic results for the larger motors are also summarized in Table 1. One motor was fired for reference at 1 *g*; a second motor was fired at 139.8 *g*; and a third at 190.1 *g*. The desired higher acceleration level (240 *g*) could not be achieved because of the high aerodynamic drag of the test installation at the end of the centrifuge boom. Pressure histories of these firings are shown in Fig. 8, with reported standard deviation ($3\sigma$) limits superimposed. Here again, the data fell well within these $3\sigma$ limits, and no drastic deviations in profile were manifested, even at 190 *g*. Therefore, within the limits of the environmental conditions to which all the test motors were subjected in this test program, scale-up from 3-lb samples to 100-lb samples did not reveal adverse acceleration effects on the performance of the test motors.

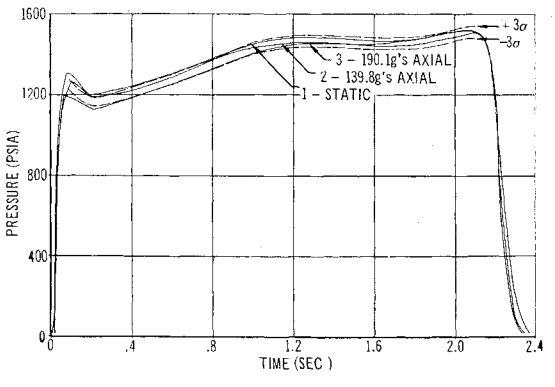


**Fig. 8 Sandia tests of 10-KS-2500 test motors.**

## Conclusions and Recommendations

This program attempted, in a gross manner, to identify a threshold for performance deviation resulting from acceleration-oriented combustion phenomena, but, for the simple test-motor configuration used, no such threshold was found. No interrelated effect of chamber pressure level and the magnitude and direction of the acceleration loading was detected, nor was there any significant difference in sensitivity due to propellant formulation or motor size. However, performance deviations were observed by others under conditions where no attempt was made to isolate the basic modes postulated here as possible causes. The test specimens were of simple configuration in order to isolate the possible cross-coupling effects between the postulated modes for the causes of the reported ballistic anomalies. Since no ballistic anomalies were detected, the thermodynamic mode, for all practical purposes, is not the predominant mechanism for the performance deviation under high acceleration loads. The question still remains as to whether the threshold for the ballistic anomalies is sensitive to the acceleration-induced mechanical forces causing significant stresses and deformation of the burning surfaces.

## Appendix

### Acceleration Effects on Head-End Pressure

The energy equation for isentropic process in high acceleration environment is represented in the following form:

$$\Delta H_s = \frac{U_2^2 - a^2t^2 - U_1^2}{2g} = C_p(T_2 - T_1) = \frac{\gamma R}{\gamma - 1}(T_2 - T_1) \quad \text{(A1)}$$

where $C_p$, $\gamma$, and $R$ are effective mean values with units as given in the Nomenclature.

The equation of state for an isentropic process is

$$T_2/T_1 = (A_1U_1/A_2U_2)^{\gamma-1} \quad \text{(A2)}$$

Solving Eq. (A1) for $T_2$, substituting for $T_2$ in Eq. (A2), and solving for $A_2$ gives

$$A_2 = \frac{A_1U_1}{U_2}\left[1 - \frac{\gamma - 1}{2g\gamma RT_1}(U_2^2 - a^2t^2 - U_1^2)\right]^{1/(1-\gamma)} \quad \text{(A3)}$$

Differentiating Eq. (A3) with respect to the velocity at station 2 gives

$$\frac{dA_2}{dU_2} = -\frac{A_1U_1}{g\gamma RT_1}\left[1 - \frac{\gamma - 1}{2g\gamma RT_1}(U_2^2 - a^2t^2 - U_1^2)\right]^{\gamma/(1-\gamma)} - \frac{A_1U_1}{U_2^2}\left[1 - \frac{\gamma - 1}{2g\gamma RT1}(U_2^2 - a^2t^2 - U_1^2)\right]^{1/(1-\gamma)} \quad \text{(A4)}$$

In this application, station 2 can be assigned to the throat of the rocket motor, and station 1 can be assigned to the head-end of the rocket-motor plenum chamber. The boundary conditions for this problem are then

$$U_1 = 0 \qquad dA^*/dU^* = 0 \quad \text{(A5)}$$

Solving Eq. (A4) with the boundary conditions for the velocity at the throat gives

$$U^* = \{[(\gamma - 1)/(\gamma + 1)][2g\gamma RT_1/(\gamma - 1)] + a^2t^2\}^{1/2} \quad \text{(A6)}$$

By combining Eqs. (A1) and (A6) with the isentropic relations,

$$T^* = T_1\{1 - [(\gamma - 1)/(\gamma + 1)][1 - (a^2t^2/g\gamma RT_1)]\} \quad \text{(A7)}$$

$$P^* = P_1(T^*/T_1)^{\gamma/(\gamma-1)} \quad \text{(A8)}$$

Equations (A6–A8) represent an isentropic expansion process without mass addition. To apply these equations to a solid-propellant rocket combustion process, mass addition must be accounted for in order to determine the equilibrium conditions. The mass rate generated is equal to the sum of the mass rate accumulated and the mass rate discharged:

$$rA_b\rho_p = [\partial(\rho_cV_c)/\partial t] + [A^*U^*P^*/RT^*] \quad \text{(A9)}$$

However, $\partial(\rho_cV_c)/\partial t$ can be neglected for equilibrium conditions, and since the standard burning-rate law for solid propellants, unmodified for erosive burning or acceleration-oriented combustion phenomena, is $r = cP^n$, then

$$rA_B\rho_p = cP^nA_b\rho_p \simeq A^*U^*P^*/RT^* \quad \text{(A10)}$$

Substituting Eq. (A8) into Eq. (A10) and solving for $P_H = P_1$ gives

$$P_H = \left[\frac{U^*(T^*/T_1)^{1/(\gamma-1)}}{c(A_b/A^*)\rho_pRT_1}\right]^{1/(n-1)} \quad \text{(A11)}$$

where $U^*$ is given by Eq. (A6) and $(T^*/T_1)$ by Eq. (A7). If the $a^2t^2$ terms in the latter parameters are neglected, the familiar form of the equation for head-end pressure is obtained:

$$P_1 = \left[\frac{[2/(\gamma + 1)]^{(\gamma+1)/[2(\gamma-1)]}(g\gamma/RT_1)^{1/2}}{c\rho_p(A_b/A^*)}\right]^{1/(n-1)} \quad \text{(A12)}$$

By examining the ratio of Eq. (A12) to Eq. (A11), a relative measure of the effect of the high acceleration environment on this parameter can be obtained. For example, for $a = 150\ g = 4824$ ft/sec$^2$, and $t = 0.1$ sec, the ratio of Eq. (A12) to Eq. (A11) for identical ballistic parameters is 1.011. Therefore, under conditions of high acceleration and long staytime, some acceleration effect should be detected on the measurement of $P_1$ with suitable instrumentation.

## References

[1] Thatcher, J. H., "Deformation of case bonded propellants under axial acceleration," Bulletin of the 20th Meeting of the JANAF-ARPA NASA Panel on Physical Properties of Solid Propellants, Vol. I (1961).

[2] Knauss, W. G., "Displacements in an axially accelerated solid propellant rocket grain," Bulletin of the 20th Meeting of the JANAF-ARPA-NASA Panel on Physical Properties of Solid Propellants, Vol. I (1961).

[3] Iwanciow, B. L., Lawrence, W. J., and Mertens, J., "The effects of acceleration on solid composite propellant combustion," AIAA Preprint 64-227 (1964).

[4] Horton, J. G., II, "Experimental evaluation of solid propellant rocket motors under acceleration loads," AIAA Preprint 64-137 (1964).